

# DELINEATION OF WATER INFLOW IN AN UNDERGROUND POTASH MINE WITH 3-D ELECTRICAL RESISTIVITY IMAGING

*Robert A. Eso, University of British Columbia, Vancouver, Canada*

*Michael Maxwell, Golder Associates Ltd., Vancouver, B.C., Canada*

*Douglas W. Oldenburg, University of British Columbia, Vancouver, B.C., Canada*

*John Unrau, Mosaic Potash, Esterhazy, Saskatchewan, Canada*

## Abstract

Delineating water inflow in underground potash mining environments has routinely been done using conventional mining methods, seismic techniques and recently GPR as a useful non-invasive tool. The combination of highly resistive dry salt and highly conductive wet salt makes these water inflow areas a good candidate for Electrical Resistivity Imaging (ERI). Mosaic Potash, Golder Associates Ltd., and the University of British Columbia's Geophysical Inversion Facility (UBC-GIF) have worked to develop and apply ERI techniques for the underground environment. Because of the 3-D distribution of current and potential electrodes and the 3-D nature of the targets, full 3-D forward modeling and inversion of the data are required. The nature of underground mining limits the placement of electrodes to existing underground drifts and this severely restricts the available electrode geometry. By placing additional electrodes in boreholes, a survey geometry with enough information to constrain the 3-D inversion can be deployed. We present a case study of the delineation of a water inflow in a potash mine using 3-D ERI. The resulting inversion models of electrical conductivity have helped to focus drilling and mitigation efforts and have provided the geotechnical engineers and mine personnel with valuable information about the underground water distribution.

## Introduction

The Mosaic Potash mine operations are located near the town of Esterhazy, Saskatchewan, Canada. The mine level is situated approximately 964 meters below the surface and mining is done using a long room and pillar method. The ore body is on average 30 meters thick with a typical composition of 55% halite, 40% sylvite, 4% carnallite and 1% insolubles (Maxwell *et al.*, 2005). Seismic techniques (Gendzwill, 1969) and underground GPR (Annan *et al.*, 1988) have been successfully employed in the underground potash mining environment. Dry salt is an electrical resistor, with apparent resistivities ranging from 100-100,000  $\Omega$ -m, but becomes very conductive when wet, with resistivities on the order of 0.01-10  $\Omega$ -m. This large contrast in electrical conductivity makes the use of ERI an attractive method for detecting water inflows.

We present a study of an application of underground 3-D ERI techniques to a real-world problem faced by mine personnel: delineating possible water bearing zones in the salt formation and in the overlying strata. The active underground mining environment contains a large number of electrical noise sources such as metallic mine infrastructure along the drifts, pumps, power stations, drilling and blasting. Prior to this study, 2-D ERI techniques were used in the underground potash environment and was consistent with GPR and seismic surveys, while test drilling verified the ERI results (Maxwell *et al.*, 2005). The survey area in this study is an intersection of two drifts with an inflow of water, shown in Figure 1. The 3-D nature of the target and the geometry of the available drifts dictate that the use of

3-D survey geometry and interpretation techniques should be used. The geometry available to place electrodes were the drifts at the intersection, three boreholes that were drilled to a height of 16m above the intersection for a cross-hole GPR survey and a 25 meter high raise that was cut into the back near the intersection. After performing a survey design procedure, we two additional boreholes were added to the West side of the study area at an elevation of 15 meters above the back of the drifts.

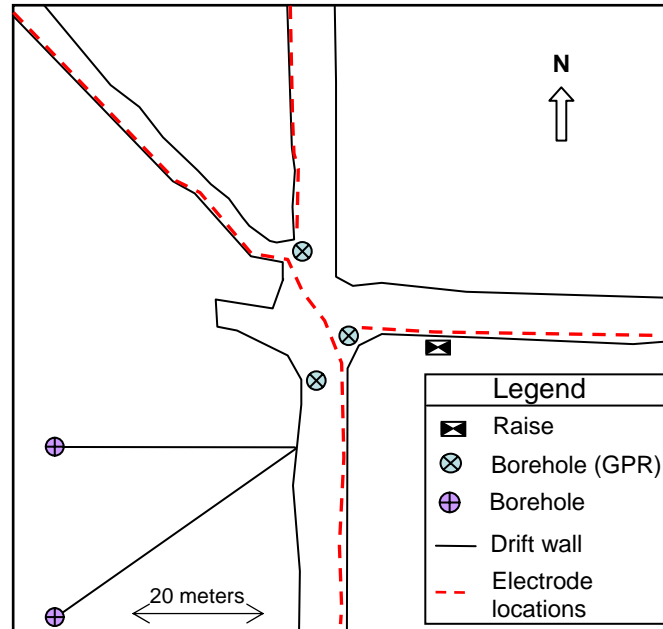


**Figure 1:** Geometry of the study area, an intersection of several mine drifts.

Numerical modeling is done using DCIP3D, a 3-D DC resistivity and IP forward modeling and inversion code developed at the UBC-GIF. The forward modeling is done using a finite volume technique and the inversion is done using a Gauss-Newton optimization to recover a minimum structure conductivity distribution that adequately reproduces the data (Li and Oldenburg, 2000). DCIP3D has been used extensively in both a mineral exploration context (Oldenburg *et al.*, 1997) and environmental and engineering geophysics (Yuval and Oldenburg, 1996). The inversion code has been parallelized to run on a standard Linux cluster using the MPI library allowing the rapid solution of very large 3-D problems.

## Survey Design

The placement of current and potential electrodes is limited to existing drifts, raises and boreholes in the underground mining environment, which can result in a survey geometry that is not well suited for recovering a 3-D conductivity distribution. Our survey design methodology can be generalized into three separate steps. It starts with forward modeling of a synthetic water model designed through *a priori* information that often incorporates knowledge and experience of mine personnel. The data resulting from this model can then be evaluated for its signal strengths characteristics. A synthetic inverse modeling study is then done to evaluate the ability for a given survey design to adequately resolve a known conductivity structure. Finally, an analysis of the sensitivity matrix is done to look for spatial regions where the survey has become less sensitive to changes in the electrical conductivity to identify possible locations to place additional boreholes for

electrodes to expand the survey geometry. This procedure can then be repeated to evaluate the benefits of modifications to the survey design.

### Synthetic Forward Modeling

A synthetic forward modeling is the beginning of our survey design methodology. A conductivity model is designed based on a hypothesis of the potential distribution of conductive material in the region. These synthetic models usually contain the geometry of the mine drifts, a background conductivity value, and an anomalous target. Figure 2 shows an example of one such synthetic model. The geometry of the mine drifts are shown in red and a synthetic conductive target is shown in blue<sup>1</sup>.

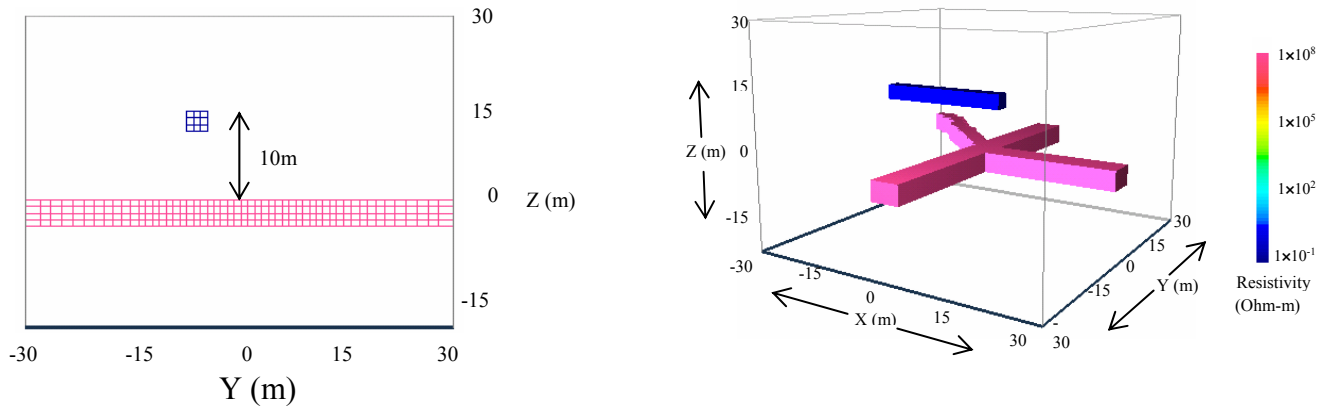


**Figure 2:** Synthetic conductivity model shown in a.) cross section showing the mesh discretization b.) 3-D perspective of the same model.

A  $300 \Omega\text{-m}$  background resistivity was chosen based on previous experience with ERI in the region. The mine drifts were modeled as resistive prisms 6 meters wide and 3 meters tall. The drift model consists of a straight passage intersecting two other drifts, one intersecting perpendicular and the other intersecting at an angle of 45 degrees. This geometry corresponds to the mine intersection shown in Figure 1. To simulate the infinitely resistive air that comprises the drifts, a conductivity of  $1 \times 10^{-8}$  was applied to those cells pertaining to the drifts<sup>2</sup>. A conductive target 25 meters long and 3 meters wide was used to simulate a water saturated salt body, and was assigned a conductivity of 10 S/m. The discretized mesh used to generate the forward model has  $1\text{m}^3$  cells in the primary region of interests. The cells slowly increment in size with increasing distance from the region of interest volume so that the assumed boundary conditions are satisfied. The total number of cells in the discretized volume was 346,560.

Once a synthetic model is created, forward modeling is used to generate the fields arising solely from the anomalous body. We evaluate

$$V_s = F[m] - F[m_0] \quad (1)$$

where  $V_s$  is the secondary potential arising solely from the conductive body,  $F[m]$  represents the synthetic data calculated for the total model, and  $F[m_0]$  represents the data calculated from the

<sup>1</sup> Our convention for displaying conductivity models is to display conductors as red, and resistors as blue as conductors in this environment are inferred to be water inflows.

<sup>2</sup> Plotting the mine drifts in the conductivity model results in a colorbar scale ranging over several orders of magnitude due to the large resistivity values used to simulate the air cells.

background model. For this example, the background model consists of a 300  $\Omega$ -m wholespace and the infinitely resistive mining drifts. The total model is comprised of the wholespace, drifts and target.

This secondary potential can be evaluated for several different array configurations to identify electrode placements that optimize signal strengths or to evaluate the ability for a given array to detect a synthetic target. For example, it was found that the strongest signal strengths were obtained from a geometry that placed transmitting currents parallel to the anomalous body. Although valuable information can be obtained through studies of the total and secondary potentials arising from a given survey geometry and assumed target, it does not address issues concerning the resolution of a given survey geometry.

### *Synthetic Inverse Modeling*

A synthetic inverse modeling study can be used to evaluate the resolving capability of a particular survey design. In this procedure, synthetic data from a conductivity model is generated and subsequently corrupted with noise to simulate collection in a noisy environment. This data is then inverted and the resulting conductivity model evaluated. Unlike inversions of field data, the true conductivity model is known, allowing the resulting models to be evaluated for how well a given survey geometry can resolve the known conductivity structure.

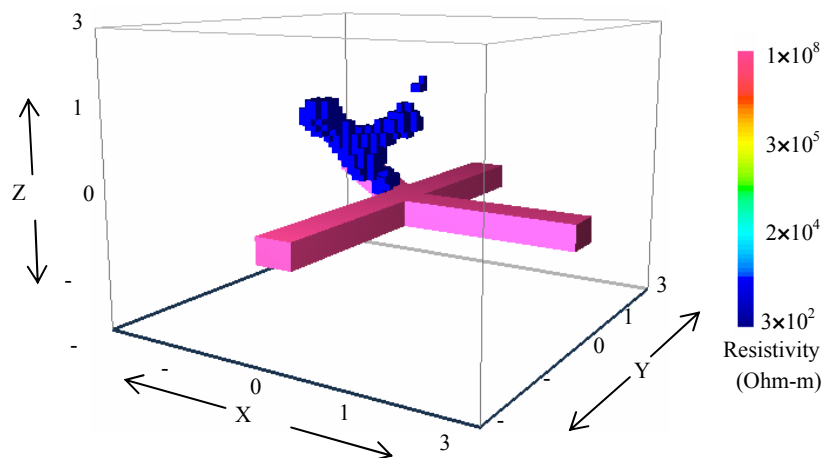


**Figure 3:** Recovered inverse model using the data generated from a dipole-dipole survey within the existing mine drifts.

Using the synthetic model shown in Figure 2, a dipole-dipole survey was simulated out in a traditional 2-D acquisition mode along the mine drifts. In this survey, essentially two dipole-dipole surveys were carried out: one along the drift in the Y-direction, and another along the drift in the X-direction, continuing straight through the intersection and along the drift intersecting at 45 degrees. The survey was conducted for a distance of 120 meters in both directions using  $a = 3$  meters and  $n = 1$  to 18. The resulting data were corrupted with 2% Gaussian noise and appropriate standard deviations assigned to each datum. The noisy data were then inverted using DCIP3D, and the resulting conductivity model is shown in Figure 3.

The recovered model shows a conductor in the same general location as the synthetic target but it also exhibits large artifacts. The artifacts and low conductivity values are likely produced because the limited survey geometry provided by the two intersecting drifts does not adequately constrain the non-uniqueness of the inverse problem. There is poor sensitivity of this dipole-dipole survey to detect the anomalous body in the synthetic model. This synthetic example serves to demonstrate the difficulty of

simply applying a known methodology that works in surface data collection to the underground environment with severely limited electrode geometry.

### Sensitivity Analysis

An important quantity necessary for the solution of the inverse problem is the sensitivity matrix. The sensitivity matrix  $J$  describes how the measured electric potential varies with perturbations to the electrical conductivity distribution, and can be written as

$$J_{ij} = \frac{\partial d_i}{\partial m_j} \quad (2)$$

where  $d_i$  is the  $i$ th potential field measurement and  $m_j$  is the logarithm of the electrical conductivity of the  $j$ th model cell. A description of the calculation of the sensitivity matrix for the 3-D DC resistivity problem can be found in Li and Oldenburg (2000). A useful quantity can be obtained by summing the sensitivity matrix, that is

$$\tilde{J}_j = \frac{1}{V_j} \sum_{i=1}^M J_{ij} \quad (3)$$

The quantity  $\tilde{J}_j$ , which we will refer to as the average sensitivity, is a measure of the total sensitivity for the  $j$ th cell normalized by its volume  $V_j$ . The average sensitivity can be viewed in 3-D in the same manner as a 3-D conductivity model.

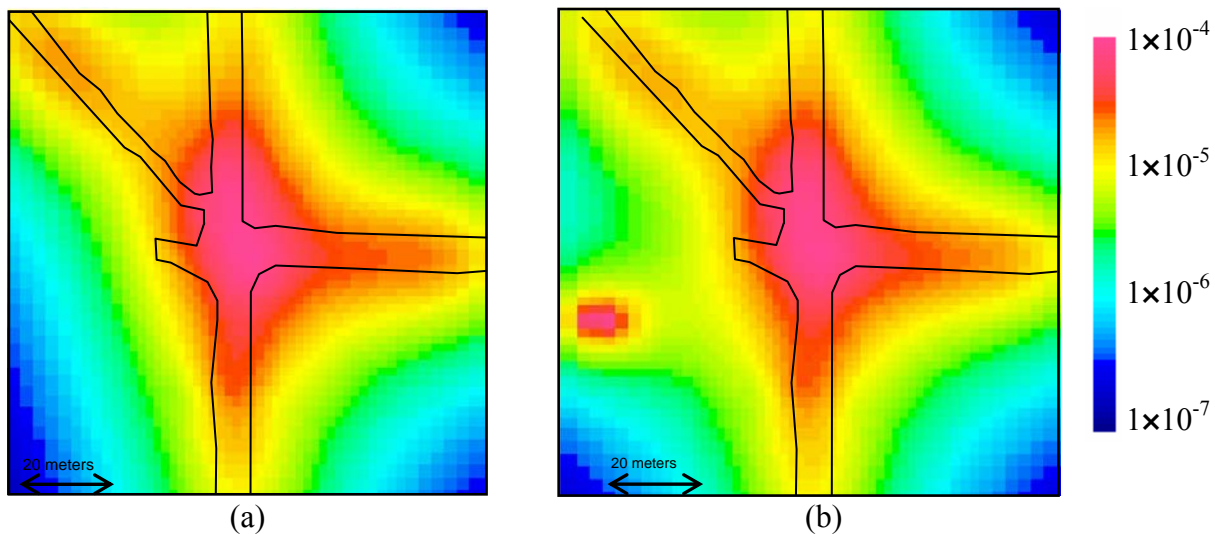


**Figure 4:** Plan view sections of the average sensitivity matrix a.) without additional boreholes b.) with one additional borehole. Units are  $V \cdot \text{Sm}^{-1} \cdot \text{m}^{-3}$ .

An example of the average sensitivity is shown in Figure 4a, where it is plotted as a plan view section in a region several meters above the mine level. The units of the average sensitivity are  $V \cdot \text{Sm}^{-1} \cdot \text{m}^{-3}$  but of more interest are its pattern and distribution than its rather than its absolute numerical value. Qualitatively, this image shows that the sensitivity is the highest closest to the electrodes and decays outwards. This result is expected, as the survey is most sensitive to changes in the conductivity near the electrodes. However, the 45 degree angle of the left-most drift results in a weaker sensitivity on

that side of the survey area, making it a good candidate for placing additional boreholes to increase the range over which the sensitivity is large. A single borehole was placed in an area exhibiting a low sensitivity value. The average sensitivity for this new configuration is shown in Figure 4b, and shows that the addition of a single borehole can greatly extend the average sensitivity away from the mine drifts.

### ***Evaluation of the survey design***

A synthetic inversion is now completed using a 3-D survey geometry and additional boreholes to constrain the model to evaluate the improvements made to the survey design through following the steps outlined above. Two boreholes in addition to the three boreholes used in the GPR survey were added to the synthetic survey design to the west of the main North-South drift, at an elevation of 15 meters above the back of the mine and can be seen in Figure 1. These boreholes were placed in order to increase the sensitivity of the survey in that area, as the near 45-degree angle of the Western drift reduces the available electrode geometry. In each of these boreholes a single electrode was placed at the end, and was used for both injecting current and making measurements of the potential.

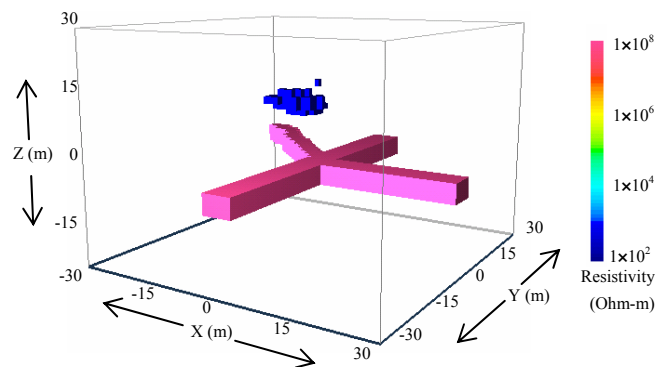


**Figure 5:** Improved synthetic inversion model obtained through a 3-D geometry and the placement of additional electrodes along boreholes.

Synthetic data were then generated using the conductivity model of Figure 2 and corrupted with 2% Gaussian noise. The model recovered from the inversion is shown in Figure 5. The improved detail in this model, compared to that of Figure 3, demonstrates the benefits of a survey design methodology that addresses issues of signal strength, resolution, and sensitivity. It is also clear that expanding the available electrode geometry using additional boreholes greatly improves the resolving power of the ERI technique. However, there a point when adding additional boreholes becomes too expensive in terms of both logistical effort and cost.

What is the optimal number of additional borehole electrodes or what is the optimal placement of additional boreholes is a difficult question to answer quantitatively. From our experience, the added logistical cost of a small number of additional boreholes is small, while greatly adding to the resolving power of the survey. We have found that good results are obtained when the additional boreholes are placed at a height above the level of the mine drifts, close to the water bearing zones, akin to a *mise-à-la-masse* survey technique.

## Results

ERI data were collected in the winter of 2004 in the Mosaic Potash Operations using the electrode layout outlined above. Data were collected using an Iris-Instruments 96 channel Syscal resistivity meter. This system allows the selection of any of the 96 attached electrodes to be used as either current electrodes or potential electrodes. Stainless steel electrodes are placed in the wall near the back or directly in back of the mine drift depending on what is easily accessible and what is the layout of mine infrastructure. Contact resistances are usually in the 0.5 k $\Omega$  – 2 k $\Omega$  range. To make electrical contact with the salt formation within the boreholes, custom-made sprint electrodes based on standard borehole centralizers are coated with conductive grease resulting in similar contact resistances. The final survey design used all 96 electrodes, with 1 electrode in each of the three GPR boreholes, and another 2 boreholes placed adjacent to the North-South oriented drift each contained a single electrode pushed to furthest end of the borehole. Approximately 16,000 quadrapole measurements were made over the intersection.

### *Data Processing*

For interpretation using DCIP3D, the measured potential voltages are first normalized to 1 Amp of current and then filtered to remove erroneous points from the dataset. One difficulty in dealing with the 3-D ERI data is that the geometry of the transmitter and potential electrodes does not lend itself to being easily plotted. In a 2-D survey, a pseudo-section can be generated allowing the interpreter to quickly gauge the quality and consistency of the data, and identify bad electrodes, as these often appear as linear features on a pseudo-section. IP and SP data are collected in conjunction with the measurements of the potential field, as we have found these to be useful in examining the quality of each data measurement. As a first pass, data exhibiting very high IP or SP anomalies are rejected, as it has been our experience that these values are usually the result of mine infrastructure and are often measured in the vicinity of pumps, power stations and ventilation fans. Additionally, data with extremely low or high apparent resistivities are rejected, as these often indicate a poor coupling between the electrode and the salt formation, or the effects of mine infrastructure. A histogram containing the number of rejected measurements is kept for all of the electrodes used in the survey. If a single electrode is associated with a large number of rejected measurements, all measurements made using any combination of that electrode are rejected. We have found this to be an effective way of quickly culling the dataset of erroneous points.

### *Inversion*

The inversion algorithm used in DCIP3D is the formulation of an objective function to be minimized, specifically

$$\phi = \phi_d + \beta\phi_m \quad (4)$$

where  $\phi$  is the objective function,  $\phi_d$  is a measure of the data misfit  $\phi_m$  is a measure of the models size and  $\beta$  is the regularization parameter controlling the tradeoff between the data misfit and model norm measurements. As a first pass, the inversion is completed using a coarse mesh discretization where cells in the region of interest are 5 meters in length. This speeds up the computation of the inversion allowing problems to be identified and inversion parameters such as the regularization parameter, background model and standard deviations to be adjusted. At this point in the processing, the misfit of each data point is evaluated. Data exhibiting very high misfits are rejected, as this means that the

inversion algorithm is trying to reduce these data in order to reduce the objective function. After the data has been pruned of erroneous data points and electrodes, the mesh discretization is reduced to increase the resolution of the inverted model.

The final inversion result using a fine mesh discretization is shown in Figure 6. This mesh uses cells of length 1.5 meters in the primary region of interest and contains a total of 1,481,544 cells. A background wholespace of 100  $\Omega$ -m as the initial and reference models was used for the inversion. The inversion contained a total of 6,531 data points and resulted in a misfit of 30,533 after 13 iterations. The inversion required 11 hours to complete the 13 iterations, with the computation distributed across 14 individual CPUs. The resulting conductivity model shows the most conductive region in the model to be to the south of the intersection at elevations between 15 and 25 meters above the mine level.

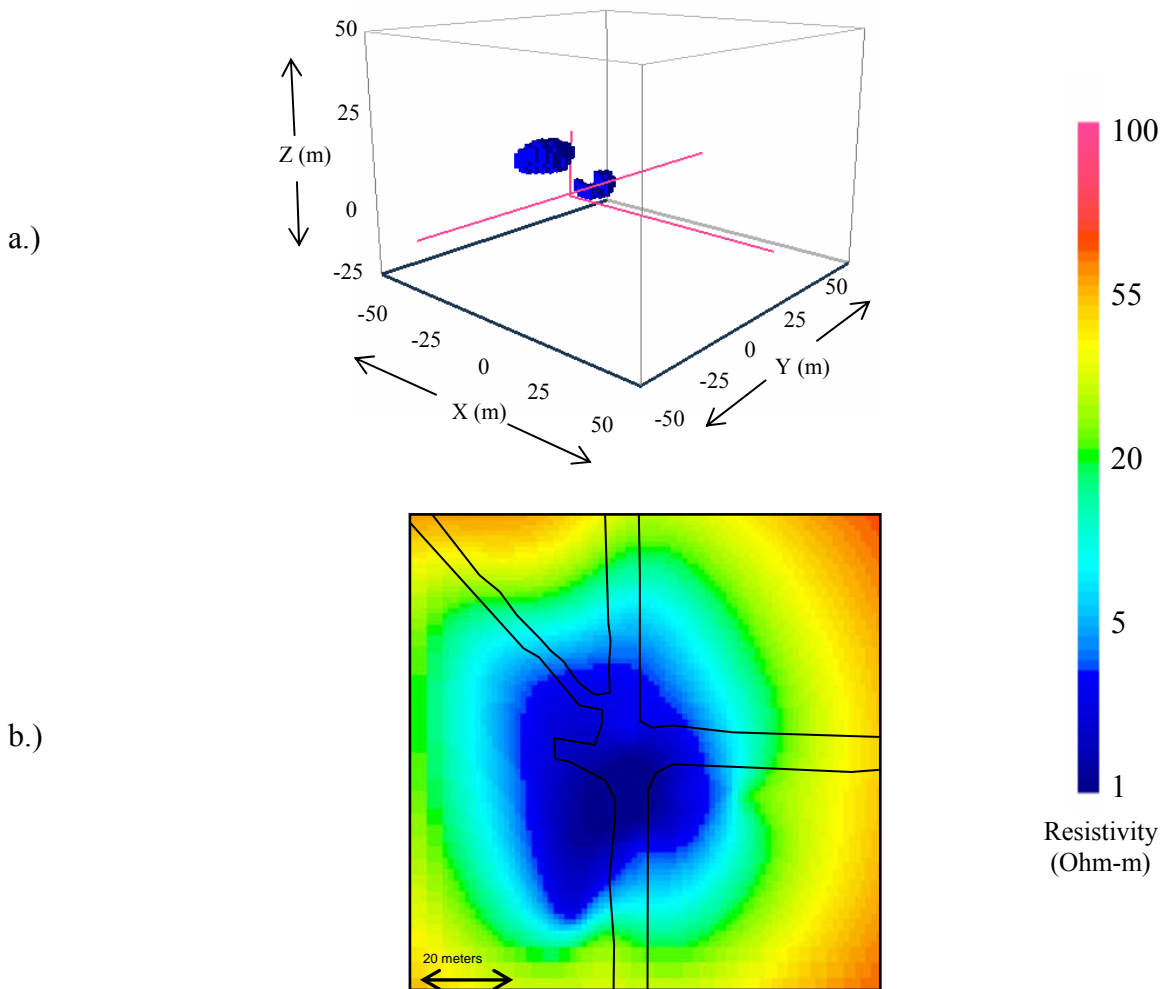


**Figure 6:** Results of 3-D ERI for the intersection. a.) iso-surface cutoff volume model showing the highest conductivity regions. The red lines indicate the location of the electrode positions in the drifts, raise and boreholes. b.) plan-view resistivity cross section taken at a height of 15 meters above the back of the mine.

## Conclusions

The UBC-GIF, Golder Associates Ltd. and Mosaic Potash have developed and applied 3-D ERI techniques in the underground potash mining environment. The often limited and complex drift geometry creates a difficulty for designing an experiment that adequately samples the volume. We have shown that through a methodology of forward modeling, synthetic inversions and sensitivity studies, it is possible to design a 3-D survey which has the ability to resolve the electrical conductivity distribution. The active underground mining environment contains numerous sources of electrical noise and careful examination of the data is required to ensure that the inversion does not try to fit erroneous measurements. We continue to develop and apply 3-D ERI techniques in the underground mining environment concentrating on quantifying the survey design process and methods to improve the inversion results.

## References

- Annan, A. P., Davis, J. L., Gendzwill, D., 1988, Radar sounding in potash mines, Saskatchewan, Canada, *Geophysics*, 53, pp. 1556-564.
- Gendzwill, D. J., 1969, Underground applications of seismic measurements in a Saskatchewan potash mine, *Geophysics*, 34, pp. 906-915.
- Li, Y., Oldenburg, D. W., 2000, 3D inversion of induced polarization data, *Geophysics*, 65, pp. 1931-1945.
- Maxwell, M., Unrau, J., Eso, R. A., Oldenburg, D.W., Song, L.P., 2005, Advancement of 2D and 3D electrical resistivity techniques for underground applications in a potash mine, Technical Paper, International Symposium on Mine Planning and Equipment Selection, Banff, 2005.
- Oldenburg, D. W., Li, Y., Ellis, R. G., 1997, Inversion of geophysical data over a copper gold porphyry deposit: a case history for Mt. Milligan, *Geophysics*, 62, 1419-1431.
- Yuval, Oldenburg, D. W., 1996, DC resistivity and IP methods in acid mine drainage problems: results from the Copper Cliff mine tailings impoundments, *Journal of Applied Geophysics*, 334, pp. 187-198.